

Experimental modeling and feedback control of a piezo-based milli-actuator

R.A. DE CALLAFON*, D.H.F. HARPER†, R.E. SKELTON AND F.E. TALKE‡

University of California, San Diego
Dept. of Applied Mechanics and Engineering Sciences
9500 Gilman Drive
La Jolla, CA 92093-0411, U.S.A.

Abstract

In magnetic disk drive actuators, requirements to record and read data at higher track densities has made mechanical resonances of the servo actuator, suspension and the head gimbal assembly a critical consideration. The application of piezo electric material in the servo actuator can be used to refine and accomplish track following in (extremely) high track density magnetic data storage by controlling the mechanical resonance modes and serving as a so-called milli-actuator. In this paper the results on the modeling and control of a piezo-based milli-actuator are presented. The modeling is done on the basis of a least squares curve fitting of an estimated frequency response and taking into account uncertainties in the modeled resonance modes of the servo actuator. The design and implementation of a robust

*Author to whom all correspondence may be addressed, email: callafon@ucsd.edu

†Now with IBM Storage Systems Division, 5600 Cottle Rd., San Jose, CA 95193

‡Center for Magnetic Recording Research at UCSD

controller provides a high bandwidth and accurate positioning of the tip of the suspension and illustrates the efficiency of the piezo-based milli-actuator.

keywords: System identification; piezoelectric; robust control; high track density recording.

1 Introduction

An unavoidable trend in magnetic recording is the aim to reduce the size or surface on which the magnetic media has to be stored. Especially, in magnetic disk drives there is an ungoing need to increase the storage capacity and areal density of the disk (Grochowski *et al.*, 1993; Grochowski and Hoyt, 1996). To avoid sacrificing fast access speed and reliability of the magnetic storage media in case of an increased areal density, the data has to be recorded and read with high speed and extreme precision on the magnetic disk.

The areal density is a combination of track density, measured in track per inch (TPI) in radial direction of the disk and bit density, measured in bits per inch (BPI) in tangential direction of the disk. For future high track density recording applications with areal densities of 10Gbit/in², the track density approaches 25kTPI, yielding a track pitch of 1 μ m and an allowable servo error of 0.1 μ m (Miu and Tai, 1995; Grochowski and Hoyt, 1996). These position requirements go beyond the possibilities of existing hard disk drive mechanisms as resonances of the structural support or flexure interfere with the position accuracy requirements.

In many of the existing hard disk drive mechanisms, a single Voice Coil Motor (VCM) actuator is used to perform the positioning of the read/write head over the disc surface. Novel design concepts such as advances in head and disk design, interface and channel technologies have allowed the improvement of the storage capacity. However, the development of a faster and more accurate servo mechanism that is able to position the read/write head with increased precision is still an active field of research (Cheung *et al.*, 1996; Koganezawa *et al.*, 1996; Horsley *et al.*, 1997; Guo *et al.*, 1998).

Most of the research is directed towards the design of so-called micro- and milli-actuators.

These actuators are used in a dual-stage concept, where the VCM is used for the gross movements, while a second (milli-) actuator is used for the fine movements of the read/write head located at the tip of the suspension. This paper shows that such milli-actuators can also be used to suppress mechanical resonance modes of the structural support or flexure that interfere with the high accuracy positioning requirements of the read/write head. In this way, an accurate and high bandwidth actuator can be obtained that is believed to explore the possibilities for high track density recording (Fan *et al.*, 1995).

The aim of this paper is to present the results on the modeling and control of mechanical resonance modes in the flexure/suspension of a hard disk servo actuator by a prototype of a piezo electric milli-actuator. The milli-actuator used in this paper is based on the principle of two piezoelectric stacks that are inserted into the E-block, behind the base of the suspension. A schematic picture of this principle is depicted in Figure 1.

FIGURE 1 HERE

As indicated in this figure, the push/pull configuration of the piezo stacks is used to achieve a radial displacement of the tip of the suspension. The advantage of this proposed design is that it does not modify the shape of the suspension itself, thereby eliminating the need for suspension redesign. We would like to stress that the aim of this paper is not to propose a new piezo-electric actuator. Instead, this paper aims at illustrating the concepts of experimental modelling and control for such a piezo-electric actuator that is able to reduce the mechanical vibrations that interfere with the high accuracy positioning requirements in high track magnetic density recording.

The outline of the paper is as follows. First, the modeling of a prototype for the milli-actuator is presented in section 2. The modeling is done by curve fitting a measured frequency response and assuming additional uncertainties in the modeled resonance modes of the suspension and actuator. In section 3, the obtained model with uncertainty is used in an \mathcal{H}_∞ -norm based optimization to design a robust feedback controller for the prototype design. To illustrate the effectiveness of the feedback controlled milli-actuator, in section 3 also the

measured closed-loop step responses are presented where the milli-actuator and read/write head suspension is applied to a rotating disk. Finally, the paper is ended by the conclusions and future research topics mentioned in section 4.

2 Modeling of milli-actuator

2.1 Prototype design

A prototype was built to study the properties of the milli-actuator and the read/write head suspension in interaction with a rotating hard disk. The prototype is used to gather experimental data for modeling purposes and to test feedback controllers being designed. Compared to the configuration depicted in Figure 1, for the prototype a slightly different design is used. A picture of the prototype being used is given in Figure 2.

FIGURE 2 HERE

In the prototype design of Figure 2, the connection of the suspension to the e-block is used as a pivoting device. The piezo stacks are attached with cyanoacrylate to the bottom of the suspension and a special e-block. The special e-block is used in order to accommodate the test platform to support the read/write head suspension over a rotating disk, whereas the bottom connection of the stacks provide easy access to the piezo stacks for experimentation purposes.

2.2 Motivation and experiments

With less than an inch in length, the suspension exhibits many (high frequent) resonance modes that interfere with an accurate positioning of the read/write head at the tip of the suspension. Without the presence of a milli-actuator, the flexibilities in the flexure or suspension have to be controlled by the single voice-coil actuator or, even stronger, might limit the servo control performance of the single voice-coil actuator. In general, the feedback

control of the voice-coil actuator is inactive in the high-frequency range, leaving the highly undamped mechanical resonance modes of the suspension unaltered.

Given the location of the (piezo-based) milli-actuator, as indicated in Figure 1 and Figure 2, it can be seen that the milli-actuator opens the possibilities to control the flexibilities in the suspension more directly. With the design of a feedback control based on the milli-actuator, the dynamic behavior of the suspension *in radial direction* can be modified to provide more accurate read/write head positioning by suppression of the resonance modes.

Obviously, for the design of a feedback controller the resonance characteristics of the suspension needs to be determined. To determine the resonance characteristics of the recording head and suspension assembly, called the head gimbal assembly (HGA), the industry uses HGA resonance testers. In such an HGA resonance tester, the HGA is subjected to vibration inputs via shaker table, whereas the tip of the suspension is monitored via a laser doppler vibrometer.

However, with the presence of a milli-actuator at the base of the suspension, the vibration inputs to test the resonance modes of the HGA can be generated by the milli-actuator. Furthermore, we are interested in controlling the position of the read/write head at the tip of the suspension. For that purpose, the experimental data to test the dynamical behavior of the milli-actuator and HGA is obtained by using a photonic probe to measure the relative displacement $y(t)$ of the read/write head located at the tip of the suspension. For excitation purposes, the piezo stacks of the milli-actuator are supplied with a random input voltage $u(t)$. The generation of the input voltage u and the measurement of the relative position y is performed by a Digital Signal Processor (DSP), as indicated in Figure 3.

FIGURE 3 HERE

The modeling of the prototype design is done via system identification techniques, where measured time domain data $\{u(t)y(t)\}$ is used to formulate a dynamical model of the piezo-based milli-actuator in combination with the flexible HGA. During the experiments, the read/write head is supported by the air bearing generated by a rotating disk.

To illustrate the attainable static displacement at the suspension tip with the prototype design, an open-loop measured step response is plotted in Figure 4. From Figure 4 it can be observed that for an 8 Volt input voltage step, an average displacement of approximately $3\mu\text{m}$ is measured at the suspension tip. However, the open-loop behavior of the milli-actuator and HGA exhibits many lightly damped resonance modes that need to be modeled and possibly controlled in order to achieve the required position accuracy of $0.1\mu\text{m}$.

FIGURE 4 HERE

Since the milli-actuator is a fast responding mechanical system and experiments can be gathered relatively easily, it is advantageous to model the milli-actuator and HGA via a frequency domain based system identification technique (Pintelon *et al.*, 1994). In such a system identification technique, a frequency response is measured and used to find a dynamical model by curve fitting the obtained frequency response. For the piezo based milli-actuator depicted in Figure 2, the frequency domain of interest lies between the 100 Hz and the 10 kHz. For this range, a frequency response will be estimated and used to construct a dynamical model for the milli-actuator and HGA.

2.3 Frequency response estimation

The experimental setup depicted in Figure 3 is used to measure the frequency response of the milli-actuator. To obtain a frequency response of the milli-actuator, the input signal $u(t)$, being the input to the piezo stacks is designed as a sum of 300 sinusoids. Formally, the input $u(t)$ is given as

$$u(t) = \sum_{k=1}^N a_k \sin(\omega_k t + \phi_k), \text{ with } N = 300 \quad (1)$$

where the frequency grid $\Omega := (\omega_1, \omega_2, \dots, \omega_N)$ is chosen such that the frequencies $f_k = \omega_k/(2\pi)$ are distributed approximately logarithmically between 100 Hz and 9 kHz.

The amplitude a_k in (1) for each sinusoid is kept constant and set to 1, while the phase ϕ_k is chosen randomly using a uniform distribution between $-\pi$ and π . In this way, a noisy signal input signal $u(t)$ is obtained with a well defined auto spectrum $S_{uu}(\omega)$ (Ljung, 1987).

The periodic input signal $u(t)$ is applied to the piezo stacks of the milli-actuator and the relative displacement $y(t)$ of the tip of the suspension is measured and stored by the DSP. The signals $u(t)$ and $y(t)$ are sampled at 20 kHz and used to estimate the cross spectrum $S_{yu}(j\omega)$ using spectral analysis (Priestley, 1981).

With the estimated cross spectrum $S_{yu}(j\omega)$ and the auto spectrum $S_{uu}(\omega)$, the frequency response $G(j\omega_k)$ of the milli-actuator can be estimated along the frequency grid Ω via

$$G(j\omega_k) = \frac{S_{yu}(j\omega_k)}{S_{uu}(\omega_k)}$$

An amplitude Bode plot of the estimated frequency response $G(j\omega_k)$ has been depicted in Figure 5.

FIGURE 5 HERE

It can be seen from Figure 5 that the milli-actuator exhibits several lightly damped resonance modes. It should be noted that the frequency response depicted in Figure 5 is measured while the read/write head at the tip of the suspension was supported by a rotating disk.

2.4 Least squares curve fitting

Given the estimated frequency response $G(j\omega_k)$ along the frequency grid $\Omega = (\omega_1, \omega_2, \dots, \omega_N)$, the aim of the frequency domain identification is to find a (discrete time) linear time invariant model P of limited complexity that approximates the data $G(j\omega_k)$. This model can be used to characterize the natural frequency and damping of the resonance modes of the milli-actuator and HGA. Additionally, such a discrete time model can be used to design a digital feedback controller to suppress the lightly damped resonance modes of the suspension and/or HGA.

To address the limited complexity, the SISO model P to be determined is parametrized in a transfer function representation

$$P(z, \theta) = \frac{b_0 + b_1 z^{-1} + \dots + b_n z^{-n}}{1 + a_1 z^{-1} + \dots + a_n z^{-n}} \quad (2)$$

where $z = e^{j\omega}$ denote the z -transform variable and

$$\theta := [b_0 \ b_1 \ \cdots \ b_n \ a_1 \ \cdots \ a_n]$$

denotes a real valued parameter of unknown coefficients in the transfer function representation given in (2). Furthermore, it can be seen from (2) that the order or complexity of the linear model can be specified with the integer value n .

The approximation of the data $G(j\omega_k)$ by the model $P(z, \theta)$ is addressed by considering the following curve fit error

$$E(j\omega_k, \theta) := [G(j\omega_k) - P(e^{j\omega_k}, \theta)]W(j\omega_k) \quad (3)$$

that needs to be minimized. In (3), $W(j\omega_k)$ denotes a scalar weighting function used to influence the curve fitting of the frequency response data.

With the definition of the curve fit error in (3), a parameter $\hat{\theta}$ is estimated by solving the following (non-linear) minimization

$$\hat{\theta} = \arg \min_{\theta} \sum_{k=1}^N E(j\omega_k, \theta) E^*(j\omega_k, \theta)$$

where $*$ is used to denote the complex conjugate transposed. A computational procedure to address this minimization is presented in de Callafon *et al.* (1996) and used in this paper to find a model $P(z, \hat{\theta})$ via a LS curve fitting.

2.5 Modeling results

Using the estimated frequency response depicted in Figure 5, the LS curve fitting described in the previous section is used to find a dynamical model of the milli-actuator and HGA. The order n of the discrete time model $P(z, \theta)$ is set to 10 in order to capture the various resonance modes present in the estimated frequency response. The weighting $W(j\omega_k)$ in (3) is set to the inverse of the data $G(j\omega_k)$ so as to minimize a relative curve fit error

$$E(j\omega_k, \theta) = \frac{[G(j\omega_k) - P(e^{j\omega_k}, \theta)]}{G(j\omega_k)}.$$

The LS curve fitting procedure of de Callafon *et al.* (1996) is used and the results have been depicted in Figure 6.

FIGURE 6 HERE

It can be observed from Figure 6 that the dominant frequency modes have been modeled accurately by the estimated model $P(z, \hat{\theta})$. The model P can be used for the design of a servo controller for the milli-actuator. However, to design a robust controller, uncertainties and product variability in the milli-actuator and HGA have to be taken into account.

2.6 Modeling uncertainties

To design a robust performing servo controller for the milli-actuator, uncertainties in the modeled resonance modes of the actuator and HGA have to be taken into account. In this paper, these uncertainties are modeled by assuming that the nominal model $\hat{P} = P(z, \hat{\theta})$ is allowed to be perturbed to a model P via a unstructured bounded multiplicative perturbation Δ (Zhou *et al.*, 1996). In this way, a set of models \mathcal{P} is found that is given by

$$\mathcal{P} = \{P \mid P = \hat{P}(1 + \Delta), \|W\Delta\|_{\infty} < 1\} \quad (4)$$

where W is stable and stably invertible frequency dependent weighting function.

In order to pursue the design of a robust controller, a choice for the weighting function W in (4) is made. The choice for W is based on the assumption that the frequency response of the nominal model \hat{P} around the zeros at 1.9 and 5.2 kHz and the two resonance modes at 2.5 and 3.5 kHz are allowed to vary. With a possible choice for the weighting filter W depicted in Figure 7 on the top, the resulting amplitude Bode plot of the models P within the set \mathcal{P} of (4) is guaranteed to lie between the dashed lines depicted in Figure 7 at the bottom.

FIGURE 7 HERE

Given the nominal model \hat{P} and the multiplicative uncertainty with the stable and stable invertible frequency dependent weighting function W in (4), a robust servo controller for the milli-actuator can be designed.

3 Control of milli-actuator

3.1 Robust control design

For the design of a controller, consider the block scheme depicted in Figure 8.

FIGURE 8 HERE

In Figure 8, the models P within the set \mathcal{P} of (4) are represented by the nominal model \hat{P} and a weighted W multiplicative uncertainty Δ . In case $\Delta = 0$, Figure 8 simply represents the feedback connection of the nominal model \hat{P} and the controller C . In that case, the map between $col(r_2, r_1)$ and $col(y, u)$ is given by the transfer function matrix $T(\hat{P}, C)$ with

$$T(\hat{P}, C) = \begin{bmatrix} P \\ I \end{bmatrix} (I + C\hat{P})^{-1} \begin{bmatrix} C & I \end{bmatrix} \quad (5)$$

where r_2 indicates the suspension tip position reference signal and r_1 a piezo voltage feed-forward signal.

For the design of a feedback controller C that robustly stabilizes the feedback connection depicted in Figure 8 for all $P \in \mathcal{P}$ given in (4), a μ -synthesis is used (Zhou et al., 1996). For that purpose, the block diagram of Figure 8 is rewritten in the standard plant configuration of Figure 9.

FIGURE 9 HERE

Most of the signals used in Figure 9 can be found back in Figure 8. Using the signal w and e to indicate respectively $col(r_2, r_1)$ and $col(y, u)$ it can be seen that G in Figure 9 is

given by

$$G = \left[\begin{array}{c|cc|c} 0 & 0 & W & W \\ \hline \hat{P} & 0 & \hat{P} & \hat{P} \\ I & 0 & I & I \\ \hline -\hat{P} & I & -\hat{P} & -\hat{P} \end{array} \right] \quad (6)$$

and consists of the previously determined nominal model \hat{P} and weighting function W . Additionally, the (performance) signals w and e can be weighted to incorporate additional performance specifications.

The standard plant configuration can be used in a μ -synthesis to design a robustly stabilizing or robustly performing feedback controller C . Subsequently, the designed feedback controller has to be reduced in order to be implementable in a DSP environment. The feedback controller C designed with the μ -synthesis toolbox (Balas et al., 1995) has a McMillan degree of 25. This can be reduced to the order of 3 (PID controller) using a closed-loop reduction technique (Wortelboer, 1993) without significant performance deterioration of the designed feedback system. The Bode plot of the final design of a 3rd order linear discrete time controller that can be implemented on the milli-actuator is depicted in Figure 10.

FIGURE 10 HERE

As can be seen from Figure 10, the designed feedback controller C has integral action and has a sharp roll-off at the area where the model uncertainty becomes larger.

3.2 Implementation of control

The experimental setup depicted in Figure 3 is used to implement the designed feedback controller on the DSP system using a sample frequency of 20 kHz. To illustrate the effect of the feedback control on the dynamical behavior of the milli-actuator and the resonance modes of the HGA, first an experimentally obtained closed-loop frequency response of the milli-actuator is presented in Figure 11.

FIGURE 11 HERE

The amplitude Bode plot in Figure 11 represent the estimated frequency response of the transfer function $P(I + CP)^{-1}C$ between suspension tip position reference signal r_2 and suspension tip displacement y in Figure 8. Similar as the previously discussed experimental results, the frequency response is estimated while the suspension is applied to a rotating disk.

Compared to the open-loop frequency response depicted in Figure 5, it can be seen that a significant reduction of the resonance modes of the HGA has been obtained. Furthermore, the milli-actuator is able to track signals up to approximately 1.5 kHz. The combination of the suppression of the resonance modes and the ability to track signals up to 1.5 kHz yields a piezo-based controlled HGA that has favourable properties for high track density recording. It should be noted that these performance conditions have been realized by a relatively simple 3rd order controller.

The suppression of the lightly damped resonance modes in the HGA by the feedback controlled piezo-based milli-actuator can also be seen from an experimentally obtained closed-loop step response. To illustrate the attainable closed-loop controlled static displacement, a closed-loop step response has been depicted in Figure 12.

FIGURE 12 HERE

Compared to the open-loop step response depicted in Figure 4, it can be seen from Figure 12 that indeed a significant reduction of the flexible modes in the suspension/HGA has been achieved. Moreover, the milli-actuator is able to achieve the position accuracy requirement of $0.1\mu\text{m}$ in the step tests and has a settling time of less than 5ms.

With respect to the achieved closed-loop bandwidth, the following remarks have to be taken into account. The closed-loop bandwidth of 1.5 kHz is remarkably fast for the milli-actuator and the suspension/HGA being used in this experiment. It can be seen from Figure 5 and Figure 11 that the closed-loop bandwidth is close to the first resonance mode of the suspension.

It should be noted that the performance of the milli-actuator and the feedback controller in terms of achievable closed-loop bandwidth is limited by the flexibilities of the suspension with its implied uncertainties. This is due to the fact that the piezo-based milli-actuator is used to rotate the suspension to achieve motion of the slider at the tip of the suspension. However, a higher closed-loop bandwidth can be obtained by using the piezo-based milli-actuator on a more recent (and shorter) suspension where the flexibilities of the suspension are higher by default. For such a smaller suspension, the same modeling and control design procedure can be used to come up with a relatively low order controller that can be used to design a high performing milli-actuator that suppresses the resonance modes in the HGA.

4 Conclusions

In this paper the results on the modeling and control of a piezo-based milli-actuator are presented. The modeling is based on an experimental data and uses frequency domain identification techniques to curve fit an estimated frequency response. Modeling uncertainties and product variability in the milli-actuator and head gimbal assembly are taken into account by assuming a weighted multiplicative uncertainty for the nominal model being estimated.

The model and suggested modeling uncertainty are used in a robust control design. The order of the designed controller is relatively low to address implementation issues of the control in a commercial digital signal processor. The implementation of the feedback controller provides a high bandwidth and accurate positioning of the tip of the suspension and illustrates the efficiency of the piezo-based milli-actuator to suppress the flexibilities in the head gimbal assembly. As such, the piezo-based milli-actuator is not only used to move the tip of the suspension but is also able to control the flexibilities in the suspension for increased position performance requirements of the read/write head.

It should be noted that the work in this paper focussed merely on the design of a feedback controller for a milli-actuator to illustrate the effectiveness of reducing resonance modes in the suspension and/or head gimbal assembly. A natural extension of this work is to include

the design of a feedback controller for the voice-coil actuator.

5 References

- Balas, G.J., J.C. Doyle, K. Glover, A. Packard and R. Smith (1995). μ -Analysis and synthesis toolbox. MUSYN Inc. and The Mathworks, Inc.
- Cheung, P., R. Horowitz and R.T. Howe (1996). Design, fabrication, position sensing, and control of an electrostatically-driven polysilicon microactuator. *IEEE Trans. on Magnetics*, Vol. 32, No. 1. pp. 122–128.
- Callafon, de, R.A., D. Roover and P.M.J. Van den Hof (1996). Multivariable least squares frequency domain identification using polynomial matrix fraction descriptions. In *Proc. 35th IEEE Conference on Decision and Control*. Kobe, Japan. pp. 2030–2035.
- Fan, L.S., H.H. Ottesen, T.C. Reiley and R.W. Wood (1995). Magnetic recording head positioning at very high track densities using a microactuator-based, two-stage servo system. *IEEE Trans. on Industrial Electronics*, Vol. 42, No. 3. pp. 222–223.
- Grochowski, E. and R.F. Hoyt (1996). Future trends in hard disk drives. *IEEE Trans. on Magnetics*, Vol. 32, No. 3. pp. 1850–1854.
- Grochowski, E., R.F. Hoyt and J.S. Heath (1993). Magnetic hard disk drive form factor evolution. *IEEE Trans. on Magnetics*, Vol. 29, No. 6.
- Guo W., T. Huang, C. Bi, K. Teck Chang, T.S. Low, X. Yao and Z. Wang (1998). A High Bandwidth Piezoelectric Suspension For High Track Density Magnetic Data Storage Devices. In *The 7th joint MMM-Intermag Conference*, San Fransisco, CA.
- Horsley, D.A., A. Singh, A.P. Pisano and R. Horowitz (1997). Angular micropositioner for disk drives. In *Proc. IEEE MEMS Workshop*. Nagoya, Japan.
- Koganezawa, S., K. Takaishi, Y. Mizoshita, Y. Uematsu, T. Yamada and S. Hasegawa (1996). A flexural piggyback milli-actuator for over 5 Gbit/in² density magnetic recording. *IEEE Trans. on Magnetics*, Vol. 32, No. 5. pp. 3908–3910.

- Ljung, L. (1987). *System Identification: Theory for the User*. Prentice-Hall, Englewood Cliffs, New Jersey, USA.
- Miu, D.K. and Y.C. Tai (1995). Silicon micromachined SCALED technology. *IEEE Trans. on Industrial Electronics*, Vol. 42, No. 3. pp. 234–239.
- Pintelon, R., P. Guillaume, Y. Rolain, J. Schoukens and H. Van hamme (1994). Parametric identification of transfer functions in the frequency domain – a survey. *IEEE Trans. on Automatic Control*, AC-39. pp. 2245–2260.
- Priestley, M.B. (1981). *Spectral Analysis and Time Series*. Academic Press, London, England.
- Wortelboer, P.M.R. (1993). *Frequency Weighted Balanced Reduction of Closed-Loop Mechanical Servo-Systems: Theory and Tools*. PhD thesis. Delft University of Technology, Delft, the Netherlands.
- Zhou, K., J.C. Doyle and K. Glover (1996). *Robust and Optimal Control*. Prentice-Hall, Upper Saddle River, New Jersey, USA.

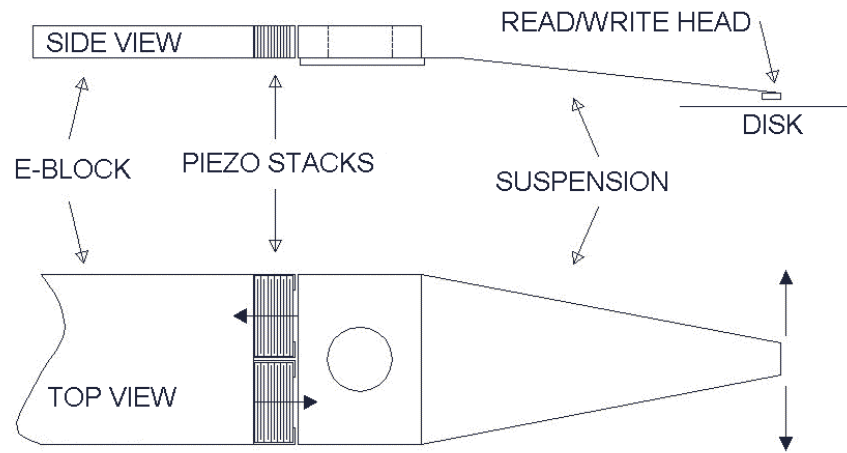


Figure 1: Principle for piezo electric milli-actuator

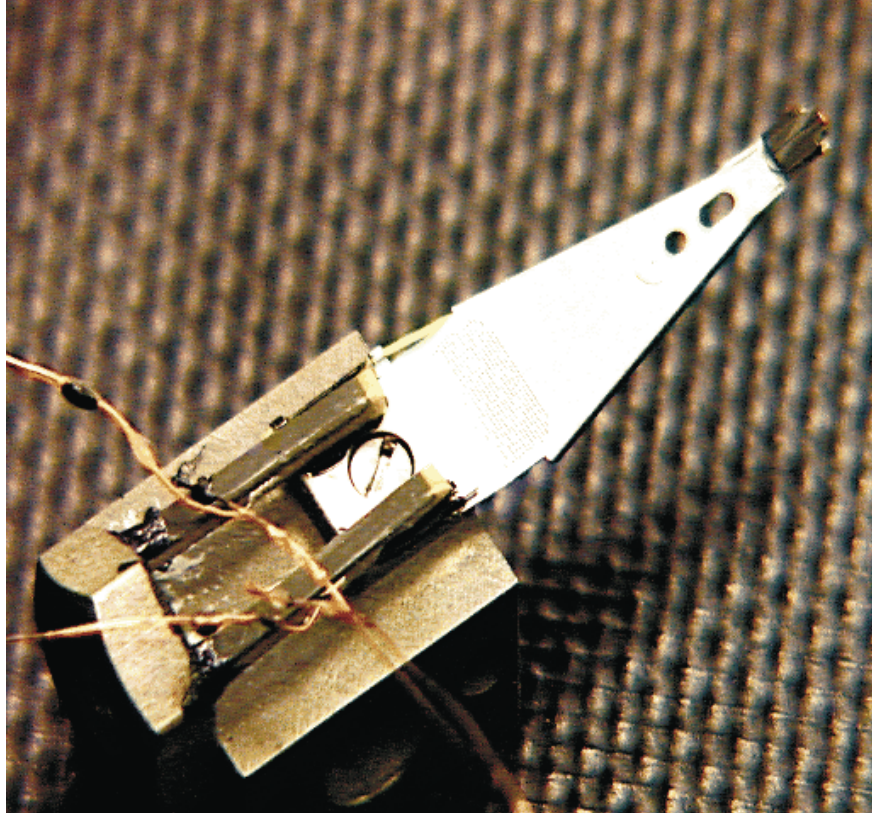


Figure 2: Bottom view of prototype with special e-block, piezo stacks, wiring and suspension of read/write head

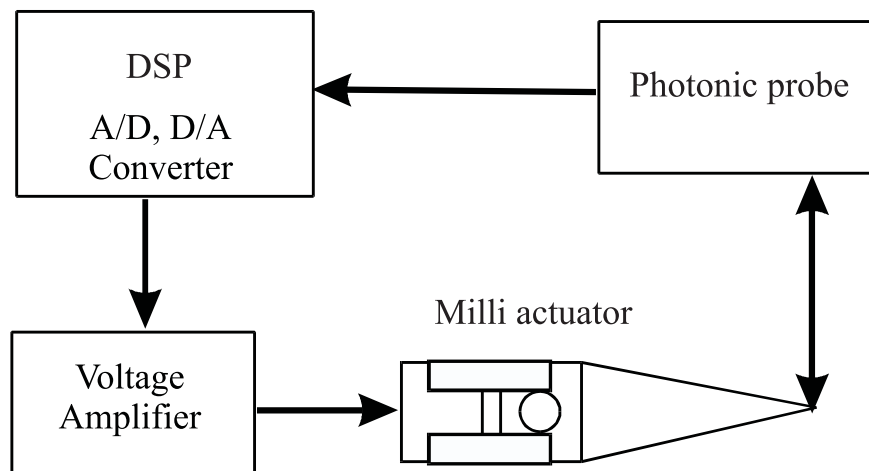


Figure 3: Experimental set up with DSP, milli-actuator, photonic probe and voltage amplifier

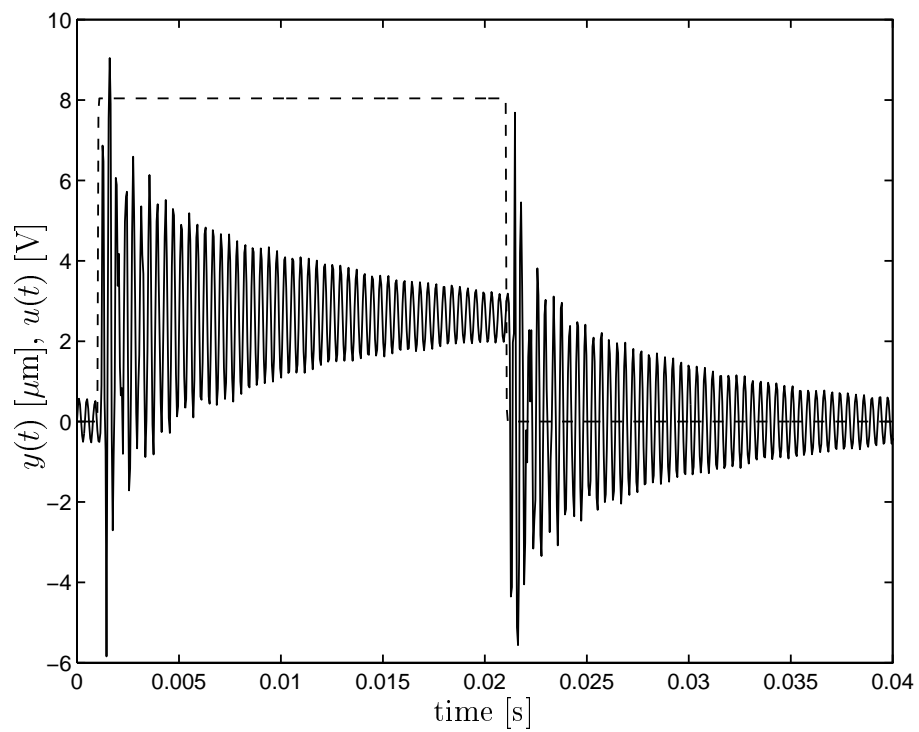


Figure 4: Measured tip position $y(t)$ in μm (—) to a step input $u(t)$ in voltage (- -)

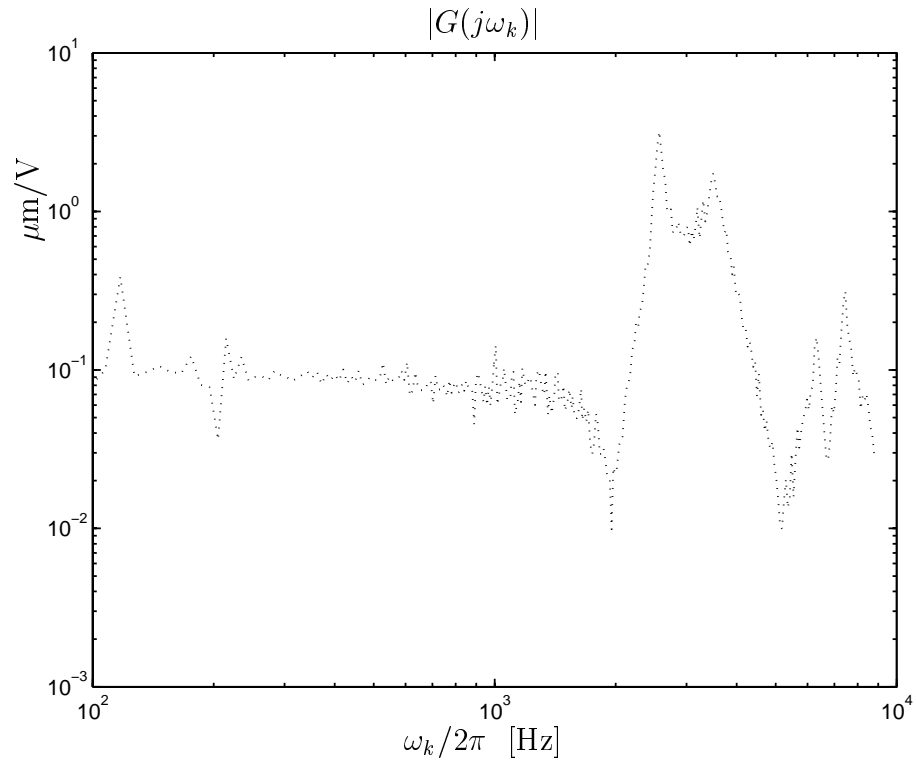


Figure 5: Amplitude bode plot of measured open-loop frequency response between piezo stack voltage and suspension tip displacement

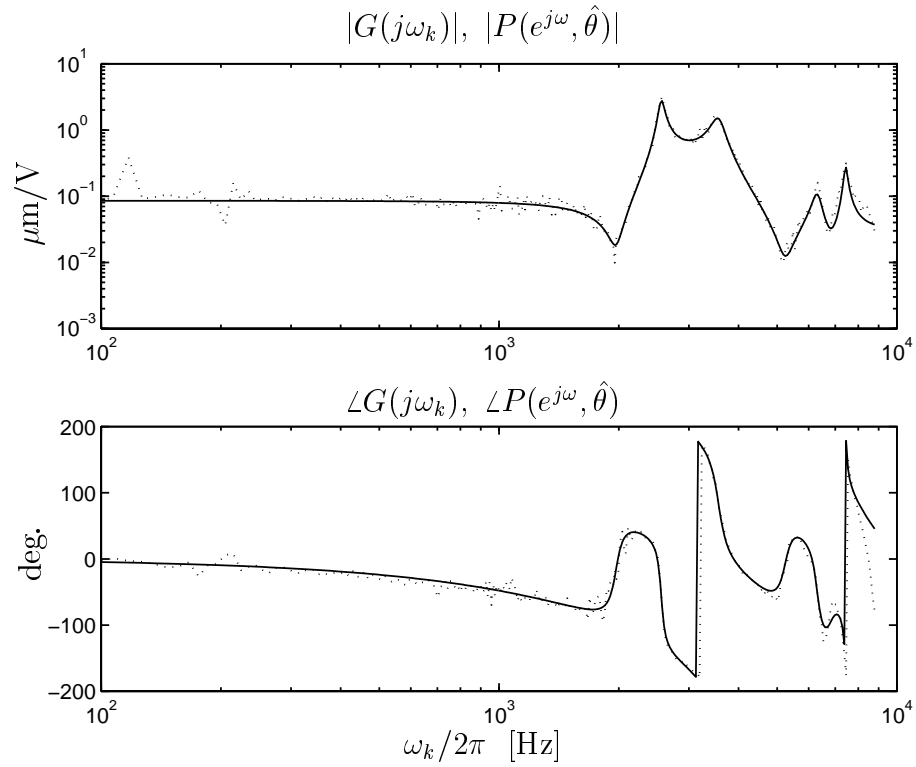


Figure 6: Bode plot of measured frequency response (dotted) and 10th order linear time invariant model (solid)

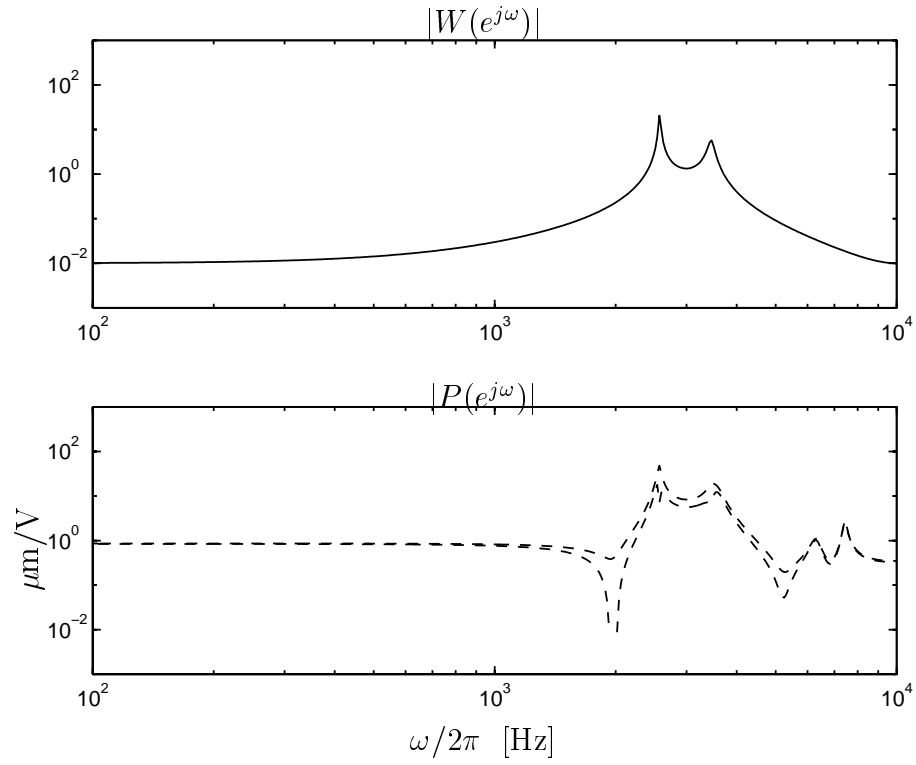


Figure 7: Weighting function W (4th order) and amplitude Bode plot range of models P in (4)

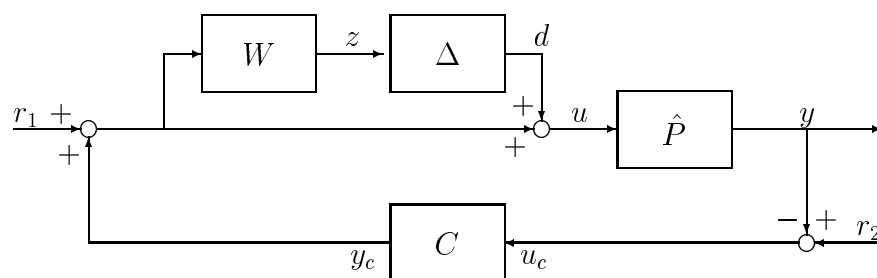


Figure 8: Feedback controller C design of nominal model \hat{P} with multiplicative uncertainty

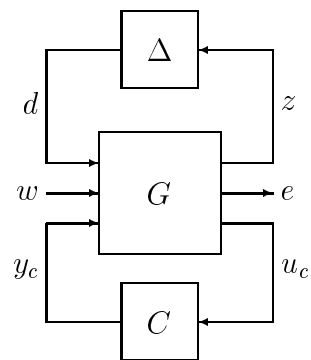


Figure 9: Standard plant configuration

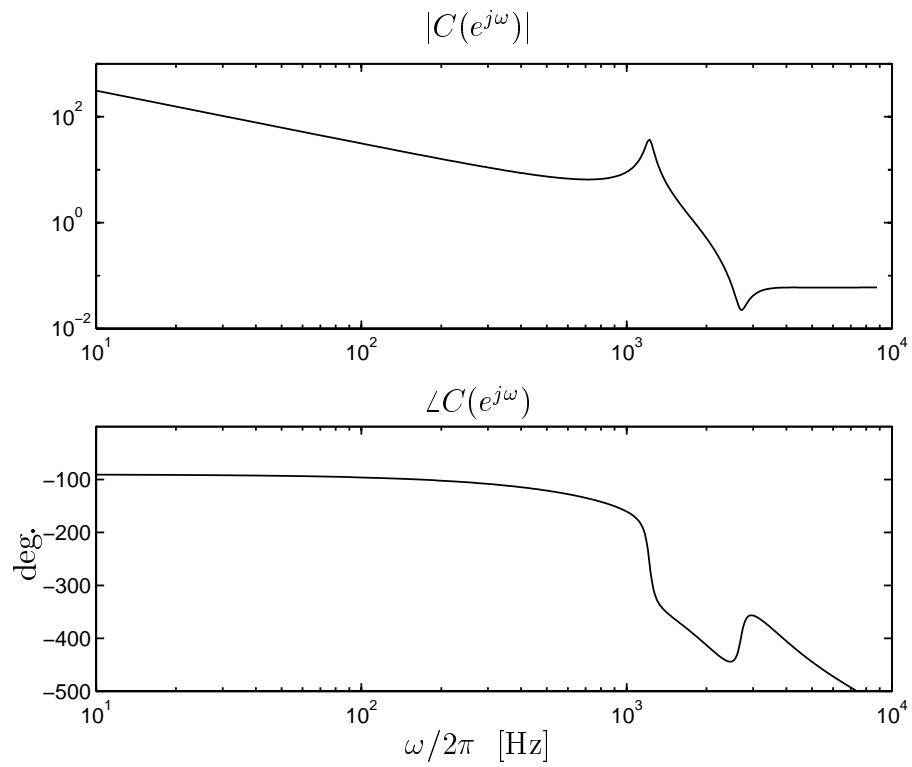


Figure 10: Bode plot of 3rd order robust linear feedback controller

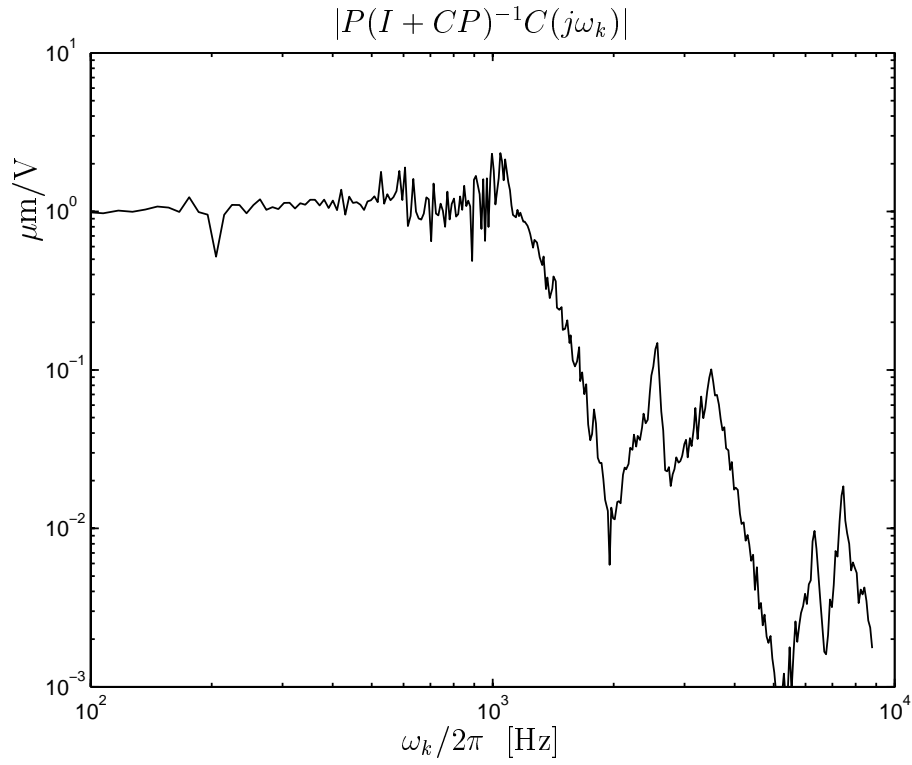


Figure 11: Amplitude bode plot of measured closed-loop frequency response between suspension tip position reference and suspension tip displacement

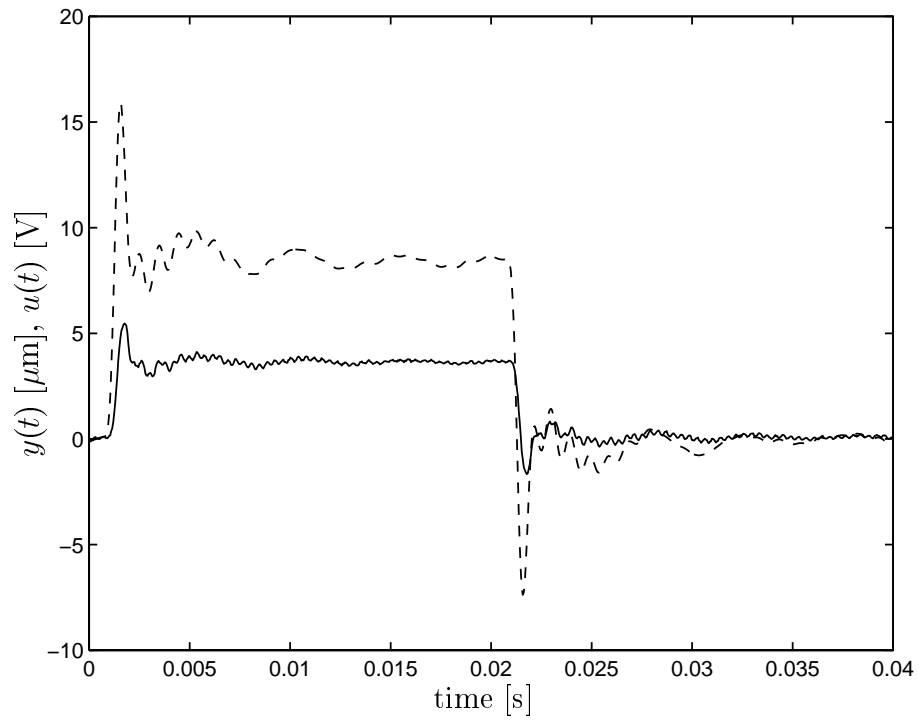


Figure 12: Measured tip position $y(t)$ in μm (—) and feedback control signal $u(t)$ in voltage (- -) to a step on suspension tip position reference signal r_2